Behavioral Model of an Analog Front-End FM-UWB using CppSim-Virtuoso

Juan C. Garcia-Gutierrez, Victor R. Gonzalez-Diaz, *Senior Member, IEEE,* and Luis A. Sanchez-Gaspariano

***Abstract*—This paper presents the design and simulation of a Frequency Modulation Ultra-Wideband (FM-UWB) transmitter and receiver operating at 125 kbps. The transmitter architecture includes a Binary Frequency Shift Keying (BFSK) sub-carrier generator, a Voltage-Controlled Oscillator (VCO), and a Power Amplifier (PA), which together enable two-level frequency modulation and transmission of the signal across a wideband channel. At the receiver side, the system integrates a regenerative demodulator designed to enhance signal recovery by suppressing unwanted noise components and improving detection accuracy. This demodulation approach contributes to maintaining a stable output, even in the presence of oscillator phase noise and other typical distortions. The complete transmitter–receiver chain is modeled and simulated using the CppSim platform, enabling accurate time-domain and frequency-domain analysis of the system behavior. The simulation results confirm the robustness of the proposed FM-UWB design, highlighting its potential for reliable wireless communication in various application scenarios. These results validate the feasibility of using FM-based ultra-wideband modulation schemes as a practical solution for short-range data transmission where signal clarity and spectral constraints are key considerations.**

Link to graphical and video abstracts, and to code: https://latamt.ieeer9.org/index.php/transactions/article/view/9750

***Index Terms*—Ultra-wideband, modulation, demodulation, sub-carrier, power amplifier, envelope detector, filter.**

I. Introduction

ULTRA-WIDEBAND (UWB) technology addresses some of the key challenges the United Nations General Assembly aims to solve for the 2030 Agenda, particularly in the areas of health and well-being, accessible and sustainable energy distribution, industrial innovation, smart cities, and the Internet of Things (IoT) technology [1]. The growing influence of IoT in daily applications drives the exploration of advanced communication protocols capable of transmitting data at a high rate with minimal power consumption. Although existing Wi-FI and Bluetooth communication protocols exhibit advantages, the emerging UWB systems solve specific constraints. UWB has distinctive characteristics that separate it from conventional protocols, and its origins date back to 1901 when Guillermo Marconi used short-duration pulses for Morse code communication. The technique was used in military applications in encrypted communications and radar systems during the 1960s. However, the Federal Communications Commission (FCC) opened UWB for public use in 2002, increasing interest in the possible applications [2], [3]. According to the FCC, the UWB definition is for $500\,\mathrm{MHz}$ signal bandwidth within a range of $10\,\mathrm{dB}$ or covers $20\,\%$ of its bandwidth around a center frequency between $3.1\,\mathrm{GHz}$ and $10.6\,\mathrm{GHz}$ while maintaining a spectral power density (PSD) not exceeding $-41.3\,\mathrm{dBm/MHz}$ [4].

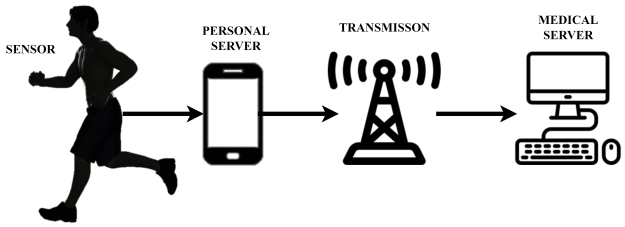

Fig. 1. Complete diagram of WBAN communication with sensors.

UWB technology receives significant attention in the biomedical field due to high data rates, low power consumption, and precise localization. These features render UWB ideal for biomedical applications, particularly in environments requiring minimal interference and high accuracy. UWB fits in WBANs (Wireless Body Area Networks) to monitor physiological signals, such as heart rate, body temperature, and glucose levels, without the need for invasive procedures (see Fig. 1). Its low-power nature extends the battery life in wearable sensors, making it suitable for ambulatory patients [5], [6]. The high precision of UWB localization (up to a few centimeters) takes advantage of hospital applications and care facilities for real-time tracking of patients and medical assets. This capability is crucial to ensure patient safety, especially for those with cognitive impairments or at risk of accidental injuries. The design of UWB transceivers for these applications is of interest to the electronics industry and research fields [7], [8]. In addition, UWB technology inherently offers low power consumption compared to traditional wireless standards, such as Wi-Fi and Bluetooth, due to its low transmission duty cycle and simple modulation schemes. These characteristics make UWB especially attractive for applications in wireless sensor networks (WSNs), WBANs, and IoT environments, where energy efficiency is critical [7].

The modeling and design of UWB transceivers lack a unique

The associate editor coordinating the review of this manuscript and approving it for publication was Roberto S. Murphy (*Corresponding author: Victor Rodolfo Gonzalez-Diaz*).

J. C. García-Gutierrez, Víctor Rodolfo González-Díaz, and L. A. Sánchez-Gaspariano are with the Faculty of Electronics Sciences, Benemerita Autonomous University of Puebla, Puebla, México (e-mails: gg223470445@alm.buap.mx, vicrodolfo.gonzalez@correo.buap.mx, and luis.sanchezgas@correo.buap.mx).

and practical synthesis. Inspired by the necessity of clarifying the UWB process design, this work proposes and describes the transceiver architecture with a specific design for FM-UWB (Frequency Modulation UWB) specifications at the system block and behavioral-model abstraction level. The contribution of this work is to serve as an initial guide to the behavioral description [9], exploiting the system-level characterization tools and their relationship with important EDA (Electronic Design Automation) tools such as Cadence-Virtuoso. Another objective of this article is to design a simple, low-complexity architecture for UWB transmission, optimized for low-power, short-range applications. This design minimizes the use of complex components, maintaining adequate performance. The FM-UWB system is modeled in C/C++ within the CppSim environment, allowing efficient simulation and functional validation at an early design stage. This approach is beneficial as it connects directly with Cadence, a tool used for designing integrated circuits, facilitating the transition from system-level modeling to physical implementation. The FM-UWB architecture description of this work is a novel configuration taking advantage of the UWB pulse forming needs and the well-known modulation schemes, tracing a simple but efficient design project for the integrated circuit design. The organization of the manuscript is as follows. Section II summarizes the frequency modulation UWB technique, using a typical architecture and synthesis of a novel receiver. Section III details the proposed FM-UWB system architecture and the construction of the behavioral model in CppSim. Section IV presents the simulation results combining the CppSim features with Cadence Virtuoso, presenting metrics for the FM-UWB transceiver and comparing them with similar transceiver architectures. Finally, Section V presents the conclusions.

II. Ultra-Wideband Frequency Modulation (FM-UWB)

A. Description of an FM-UWB Transmitter

FM-UWB Modulation is an analog spread-spectrum technique conceived from BFSK (Binary Frequency Shift Keying). In recent years, FM-UWB transmitters have seen minimal changes due to their high quality combined with low hardware costs. A typical FM-UWB implementation consists of three main blocks: a triangular wave generator (sub-carrier), a voltage-controlled oscillator (VCO), and a power amplifier (PA). The sub-carrier modulates the VCO with a triangular wave between $1\,\mathrm{MHz}$ and $10\,\mathrm{MHz}$, producing the FM-UWB signal. The resulting FM-UWB signal is therefore [10]:

$$S_{UWB}(t) = A\ cos\left(w_c t + \phi(t)\right) \tag{1}$$

Where w_c is the center frequency and $\phi(t)$ represents the frequency change. According to the definition, the signal must have a minimum of $500\,\mathrm{MHz}$ in bandwidth. Fig. 3 shows the behavior of the modulated signals for each stage.

B. Description of an FM-UWB Receiver

Unlike FM-UWB transmitters, FM-UWB receivers adopt various topologies, including delay-line demodulators at RF,

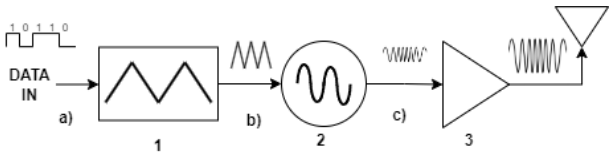

Fig. 2. FM-UWB stages: signal (a) is the input data, (b) the triangular waveform, and (c) the modulated FM-UWB output.

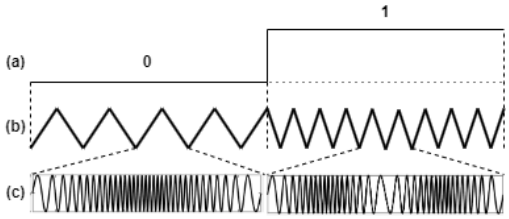

Fig. 3. The signal flow in an FM-UWB transmitter includes: (a) the input binary data, (b) a triangular sub-carrier waveform, and (c) the FM-UWB output from the VCO, where the sub-carrier modulates the carrier frequency for transmission.

regenerative demodulators, baseband delay-line demodulators, and dual-band pass-filter demodulators [11]. This work implements the proposed topology using a regenerative demodulator. This circuit is commonly used in electronic communications for demodulating modulated signals, particularly in amplitude modulation (AM) and frequency modulation (FM) systems. Regenerative demodulators became popular in the early days of radio due to their simplicity and efficiency [12]. Fig. 4 illustrates an FM-UWB regenerative demodulator, operating in the following manner:

- A Low-Noise Amplifier (LNA) amplifies the signal received from the antenna while minimizing noise interference.
- A Low Pass Filter (LPF) or High Pass Filter (HPF) attenuates unwanted frequency components.
- An Envelope Detector (ED) converts the amplitude-modulated (AM) signal into a frequency-modulated (FM) signal.

The output from the regenerative demodulator is then directed to an Analog-to-Digital Converter (ADC) or a subsequent demodulation stage for further processing.

III. The Proposed FM-UWB Transceiver Architecture

Fig. 5 illustrates a block diagram of a wireless FM-UWB transceiver.

Transmitter:

- **Data input:** The system starts sending bits.
- **Sub-Carrier Modulation**: Data are modulated using a sub-carrier, specifically a triangular wave.
- **VCO (Voltage-Controlled Oscillator)**: The VCO generates a carrier signal, with frequency changing according the modulated input voltage. The VCO phase noise, modeled as a non-linearity, is about $-70\,\mathrm{dBc/Hz}$ at 1 MHz offset. This phase noise impacts the spectral purity

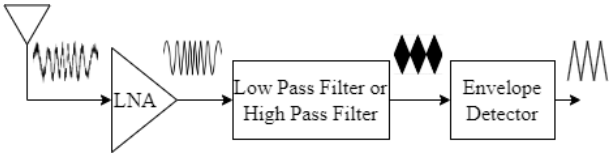

Fig. 4. FM-UWB receiver architecture: regenerative demodulator.

of the FM-UWB signal and represents a key impairment source. Incorporating it into the behavioral model.

- **PA (Power Amplifier):** up converts the modulated signal ensuring strength for transmission. A typical implementation is an power-up RF converter.

Receiver:

- **LNA (low noise amplifier):** The received signal contains low-power, the low noise amplifier improves the signal quality while minimizing added noise.
- **First-order filter**: A first-order filter cancels undesirable high-frequency components from the signal.
- **Envelope detector**: This component detects modulated signal envelope, allowing the original data to be extracted from the carrier signal.
- **Second-order Butterworth filter:** A second-order Butterworth filter further enhances the signal, improving clarity and reducing noise.
- **Envelope detector (final stage):** The second envelope detector extracts the final base-band signal.
- **Subtractor and comparator:** This block processes the extracted signal, combines, and sends output data.

A. Proposed Architecture for an FM-UWB Transmitter

The proposed transmitter (see Fig. 6) includes three main blocks: the first block is a sub-carrier generator circuit that modulates binary data input into triangular analog sub-carrier signals with two different frequencies. The second block is a VCO circuit (voltage-controlled oscillator), which translates the input triangular signals to higher frequency levels, creating a constant envelope UWB signal. The third block is a power amplifier circuit adjusting the UWB output signal, rendering it suitable for transmission. The transmitter bandwidth is of $4\,\mathrm{GHz}$ to $6\,\mathrm{GHz}$. This work shows the system model and simulation in CppSim. For the block construction and simulation configuration, refer to [9].

1) Triangular Oscillator: A sub-carrier is a digital modulator whose primary function is to convert **n** bits into triangular waves at **n** frequencies. Depending on its implementation, it can perform various types of digital modulation. CppSim tools allow a simulation of triangular waves based on their mathematical description. Equation 2 describes a triangular wave. So, code 1 details the triangular wave implementation.

$$v_{tri}(t) = \frac{4A}{T}\left|t - \frac{T}{2}\left(2\left\lfloor\frac{t}{T}+\frac{1}{2}\right\rfloor+1\right)\right| - A \qquad (2)$$

Where:

1) A is the maximum amplitude.
2) T is the sampling period, defined as $T = 1/f$, where f is frequency.
3) t is a continuous-time variable.

The proposed triangular oscillator encodes the stream binary data input (IN) at a baud rate of $125\,\mathrm{kbps}$ into a triangular sub-carrier signal of two different output frequencies: $1\,\mathrm{MHz}$ when IN = '0' and $2\,\mathrm{MHz}$ when IN = '1'.

CppSim Code 1 Sub-carrier

```
1: Module: Sub-carrier
2: Parameters: double amplitude, double frequency
3: Inputs: double in
4: Outputs: double out
5: Static Variables: double phase_step, double phase
6: Code:
7: phase_step = frequency
8: phase = phase + phase_step
9: if phase ≥ 0.5 then
10:   phase = phase - 1.0
11: end if
12: out = 4.0 × amplitude × fabs(phase) - amplitude
```

2) Voltage Controlled Oscillator (VCO): A voltage-controlled oscillator (VCO) is an electronic device generating a periodic signal with voltage-controlled frequency. The VCO oscillation frequency varies as a function of the applied voltage, allowing to adjust the output frequency [13]. Equation (3) describes the ideal behavior.

$$v_{VCO}(t) = A\ \cos\left(w_{out}t\right) \qquad (3)$$

- $w_{out} = K_{VCO}V_{cont} + w_0$, where K_{VCO} is the VCO gain (with units of $(\mathrm{rad/s})/\mathrm{V}$ or $\mathrm{Hz/V}$) and w_0 is the VCO central free-running frequency.

The VCO characteristics in this system are:

- $K_{VCO} = 2\,\mathrm{GHz/V}$.
- $w_0 = 4\,\mathrm{GHz}$.

The CppSim Code 2 details the VCO behavioral model, and Fig. 8 shows the voltage-frequency curve for the respective K_{VCO}.

CppSim Code 2 VCO

```
1: Module: VCO
2: Parameters: double freq, double kvco
3: Inputs: double vctrl
4: Outputs: double_interp squareout, double sineout
5: Static Variables:
6: Classes: Vco vco("fc + Kv*x", "fc,Kv,Ts", freq, kvco, Ts);
7: Code:
8: vco.inp(vctrl);
9: squareout = vco.out;
10: sineout = sin(vco.phase);
```

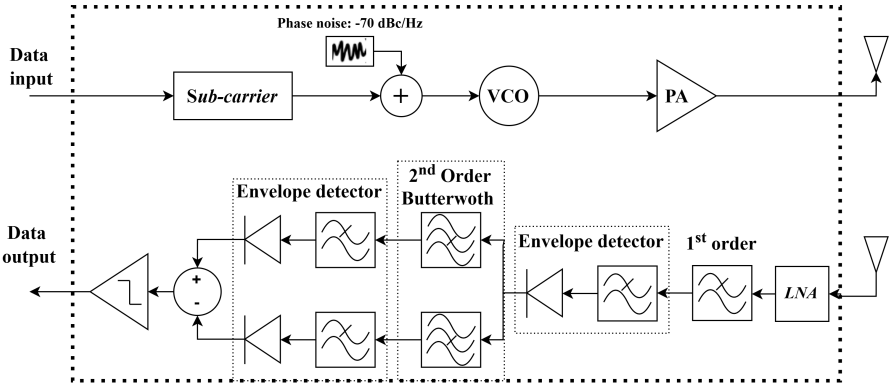

Fig. 5. Schematic representation of the CppSim model with the proposed scripts.

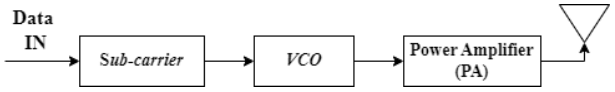

Fig. 6. The proposed FM-UWB transmitter.

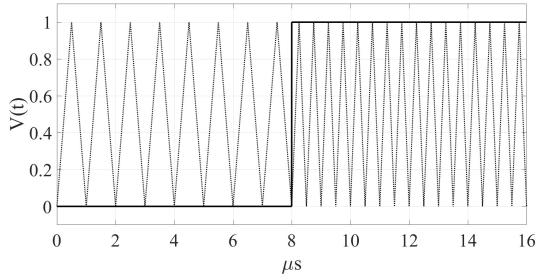

Fig. 7. Sub-carrier waveform used for data modulation.

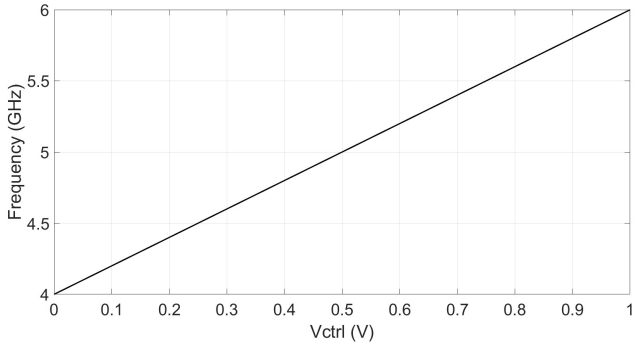

Fig. 8. KVCO curve of the designed VCO, illustrating the frequency variation as a function of the control voltage.

3) Power Amplifier: The implementation of a power amplifier (PA) relies on two key factors: the load, which in RF systems is typically set to a load impedance of $Z = 50\,\Omega$, and energy efficiency [13]. When simulating in CppSim, the noiseless power amplifier is a gain stage. To achieve the UWB characteristics, the PA output peak-to-peak voltage (V_{pp}) must not exceed $160\,\mathrm{mV}$.

B. Proposed Architecture for an FM-UWB Receiver

The proposed FM-UWB demodulation receiver (see Fig. 9) utilizes two separate demodulators:

1) FM-UWB regenerative demodulator.
2) Binary Frequency Shift Keying (BFSK) demodulator.

FM-UWB Demodulator.

The regenerative demodulator contains the following elements:

1) Low Noise Amplifier (*LNA*): Provides a $13\,\mathrm{dB}$ gain, corresponding to a scaling factor of 5.
2) First-Order Low-Pass Filter (*LPF*): Designed for a $4\,\mathrm{GHz}$ cut-off frequency with a scaling factor of 5. Equation 4 describes the first-order low-pass filter transfer function, where w_0 is the cut-off frequency and G is the system gain. Code 3 represents the implementation of a first-order LPF.

$$H(s) = G\frac{w_0}{s + w_0} \tag{4}$$

3) Envelope Detector (*ED*): This component consists of two elements:
   - A rectifier.
   - A low-pass filter with$10\,\mathrm{MHz}$ cutt-off frequency and an amplification factor of 10.

CppSim Code 3 First Order Low-pass

```
1: Module: First Order Low-pass
2: Parameters: double fp, double gain
3: Inputs: double in
4: Outputs: double out
5: Classes:          Filter filt("G", "1 +
   1/(2πw0)*s", "G,w0,Ts", gain, w0, Ts);
6: Code:
7: filt.inp(in);
8: out = filt.out;
```

BFSK demodulator

The BFSK demodulator consists of the following components:

1) Two Second-Order Band-Pass Filters (BPFs): these are Butterworth type using equation (5), with a cut-off frequency of $1\,\mathrm{MHz}$, $2\,\mathrm{MHz}$ and gain factor of 5. Equation (5) describes

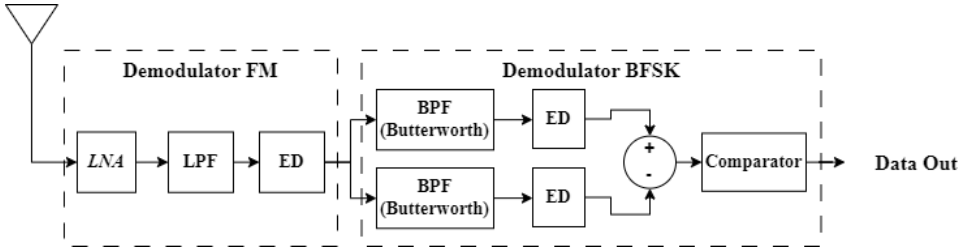

Fig. 9. Architecture of the proposed FM-UWB receiver with regenerative demodulator.

the transfer function of a second-order band-pass filter, where w_0 is the cut-off frequency, G is the gain, and Q is the quality factor. For a Butterworth filter, the quality factor is 0.7.

$$H(s) = G\frac{(w_0/Q)s}{s^2 + (w_0/Q)s + w_0^2} \tag{5}$$

2) Two Envelope Detectors (EDs): Comprises two elements:

- A rectifier.
- A second-order low-pass Butterworth filter with a cut-off frequency of $100\,\text{kHz}$ and a gain factor of 10.
  Equation (6) describes the transfer function of a second-order low-pass filter.

$$H(s) = \frac{w_0^2}{s^2 + (w_0/Q)s + w_0^2} \tag{6}$$

Codes 4 and 5 detail a second-order low-pass and band-pass filters. These codes define a module for a second-order Butterworth filter. The description requires parameters: gain and w_0 (the cut-off angular frequency), with an input signal (`in`) and outputs the filtered signal (`out`). The filter description uses a `Filter` class, instantiated with a transfer function where the numerator is $G \cdot (2\pi w_0)^2$ or $(2\pi w_0/0.7)s$ and the denominator is $s^2 + \frac{2\pi w_0}{0.7}s + (2\pi w_0)^2$. Parameters include G (gain), w_0 (cut-off frequency), and T_s (sampling period). The filter provides results through filt.out.

CppSim Code 4 Low-pass Butterworth filter

```
1: Module: Low-pass Butterworth filter
2: Parameters: double gain, double w0
3: Inputs: double in
4: Outputs: double out
5: Classes:
6: Filter filt("G*(2π*w0)^2", "s^2 +
   (2π*w0/0.7)s + (2π*w0)^2", "G,w0,Ts",
   gain, w0, Ts);
7: Code:
8: filt.inp(in);
9: out = filt.out;
```

3) Subtractor: Code 6 defines a subtractor module in CppSim. This module accepts two input signals, `v1` and `v2`, both of type `double`, and calculates their difference as the output signal (`out`).

CppSim Code 5 Band-pass Butterworth filter

```
1: Module: Band-pass Butterworth filter
2: Parameters: double gain, double w0
3: Inputs: double in
4: Outputs: double out
5: Classes:
6: Filter filt("(2π*w0/0.7)s", "s^2 +
   (2π*w0/0.7)s + (2π*w0)^2", "G,w0,Ts",
   k, w0, Ts);
7: Code:
8: filt.inp(in);
9: out = filt.out;
```

CppSim Code 6 Subtractor

```
1: Module: subtractor
2: Parameters:
3: Inputs: double v1, double v2
4: Outputs: double out
5: Static Variables:
6: Classes:
7: Code:
8: out = v2 - v1;
```

4) Comparator: Finally, code 7 represents a comparator. It takes an input signal, `in`, and compares its value with zero as the output signal (`out`). The input changes with digital values `out = 0 or 1`.

CppSim Code 7 Comparator

```
1: Module: Comparator
2: Parameters: double threshold
3: Inputs: double in
4: Outputs: double out
5: Code:
6:   if (in > threshold)
7:     out = 1;
8:   else
9:     out = 0;
```

IV. Results and Discussions

This Section presents the results of the transmitted and received data obtained from the proposed system at the behavioral level, in compliance with FCC regulations.

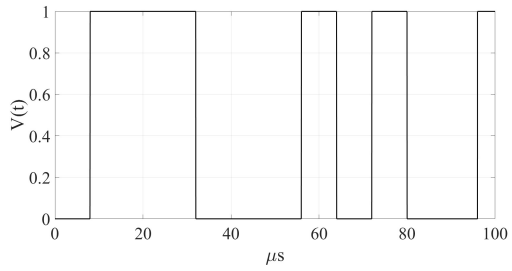

Fig. 10. Transmitted data sequence simulated over 100 µs at 125 kbps.

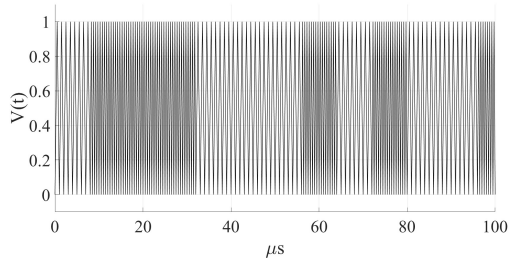

Fig. 11. Sub-carrier signal with frequencies of 1 MHz,2 MHz.

A. Transmitter

Fig. 10 shows the input data at a baud rate 125 kbps. The signal has an amplitude of V_{pp} = 1 V. When the sub-carrier modulates the signal (see Fig. 11), it transforms into two triangular waves with frequencies of 1 MHz and 2 MHz, respectively. First, the signal converts to a sine wave with a change of constant frequencies. Then, the PA scales the amplitude signal up to $V_{pp} = 160\,\mathrm{mV}$. Fig. 12 shows the resulting Power Spectral Density (PSD) from the transmitter output. The blue line represents the transmitted data PSD with maximum power between 4-6 GHz in a range of $10\,\mathrm{dBm/MHz}$. The black dotted line corresponds to the mask spectrum imposed by the FCC for UWB devices. This mask establishes the maximum permitted power emission limits in different frequency bands to avoid interference with other radio frequency services. It likely corresponds to the indoor UWB mask, allowing up to $-41.3\,\mathrm{dB/MHz}$ from 3.1 GHz to 10.6 GHz. The calculation of the PSD for the PA's output is performed using equations (7) and (8).

$$X(f) = \mathrm{FFT}(x(n)) \tag{7}$$

$$P(f) = \frac{|X(f)|^2}{N} \tag{8}$$

where:

- $x(n)$ es the discrete signal with sample index n.
- FFT is Fast Fourier Transform.
- N is the number of samples of the signal.

It is necessary to change the units, and equation 9 normalizes these units to those specified by the FCC.

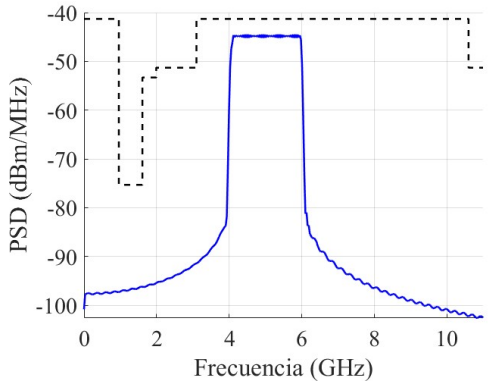

Fig. 12. PSD of the power amplifier. The black dashed line shows the FCC mask for UWB devices.

$$\begin{aligned} P_{(\mathrm{dB_W/Hz})} &= 10\log_{10}\left[P_{(\mathrm{V^2/Hz})}/Z\right] \\ P_{(\mathrm{dBm/Hz})} &= P_{(\mathrm{dB_W/Hz})} + 30 \\ P_{(\mathrm{dBm/MHz})} &= P_{(\mathrm{dBm/Hz})} + 60 \\ P_{(\mathrm{dBm/MHz})} &= 10\log_{10}\left[P_{(\mathrm{V^2/Hz})}/Z\right] + 90 \end{aligned}$$

$$P_{(\mathrm{dBm/MHz})} = 10\log_{10}\left[P_{(\mathrm{V^2/Hz})}/Z\right] + 90 \tag{9}$$

Where:

- The impedance Z in an antenna system is typically $Z = 50\,\Omega$ in radio frequency applications.

Table I displays the characteristics of the proposed FM-UWB transmitter, indicating which parameters comply with FCC regulations. Note that the transmitter complies with the FCC requirements.

TABLE I
COMPLIANCE OF THE PROPOSED FM-UWB SYSTEM WITH FCC SPECTRAL REGULATIONS

Parameter	This Work	FCC Limit	Compliant
Frequency range	4 GHz–6 GHz	3.1 GHz–10.6 GHz	Yes
Bandwidth	2 GHz	$\geq$ 500 MHz	Yes
Max PSD	$-45\,\mathrm{dBm/Hz}$	$-41.3\,\mathrm{dBm/Hz}$	Yes

B. Receiver

Fig. 13 shows the demodulated signals. The process begins with the Low-Noise Amplifier (LNA), which amplifies the incoming signal while keeping the noise level to a minimum. This amplification is crucial for enhancing the signal strength without causing significant distortion or interference. Next, a Low-Pass Filter (LPF) selectively attenuates incoming signal high-frequency components. By filtering out these unwanted frequencies, the LPF output transfers amplitude variations resembling a triangular waveform. At the final stage, the Envelope Detector (ED) converts the alternating current (AC) signal to triangular wave characteristics, providing a clear representation of the original modulation.

Fig. 14 illustrates the signal after two Band-Pass Filters (BPF), centered at 1 MHz and 2 MHz, respectively. Each BPF

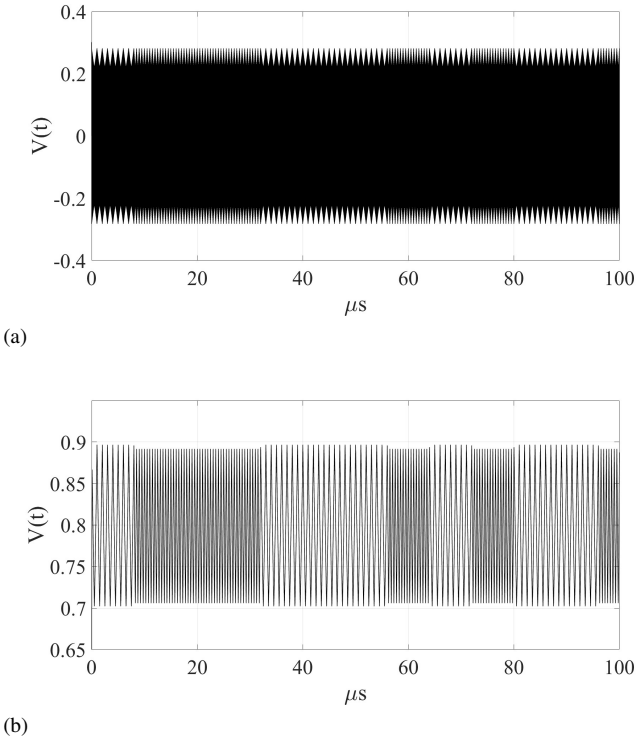

Fig. 13. Output response of the regenerative demodulator to FM-UWB signals. (a) Output signal of a 4 GHz 1st-order low-pass filter, (b) Output signal of the envelope detector.

is specifically designed to isolate the corresponding frequency component to its center frequency, effectively separating the desired spectral components from the surrounding noise and irrelevant frequencies. As a result, the output of each filter consists of two distinct spectral signals, each corresponding to the filtered frequency band.

Subsequently, these filtered signals are processed by an Envelope Detector (ED). The ED performs the critical function of converting the alternating current (AC) components of the filtered signals into low-frequency components. This transformation simplifies the subsequent decoding process as the resulting signals are steady and easier to interpret. The common mode cancellation isolates and converts key frequency components, and the system facilitates the accurate extraction and decoding of the original information encoded within the signal. This combination of filtering and envelope detection ensures high fidelity in the demodulation process, minimizing distortions and preserving the integrity of the transmitted data.

Fig. 15 shows the subtraction of $V_1 - V_2$, effectively reducing noise by canceling the signals of the common-mode present on both inputs. This subtraction improves signal quality, leaving a cleaner differential signal. The resulting output goes through the comparator with a reference set to ground. The comparator processes the input signal and generates a digital output, representing the recovered data.

C. Transceiver Input and Output Data

Fig. 16 displays the transient analysis of a transmitted digital signal and the corresponding received pattern with the

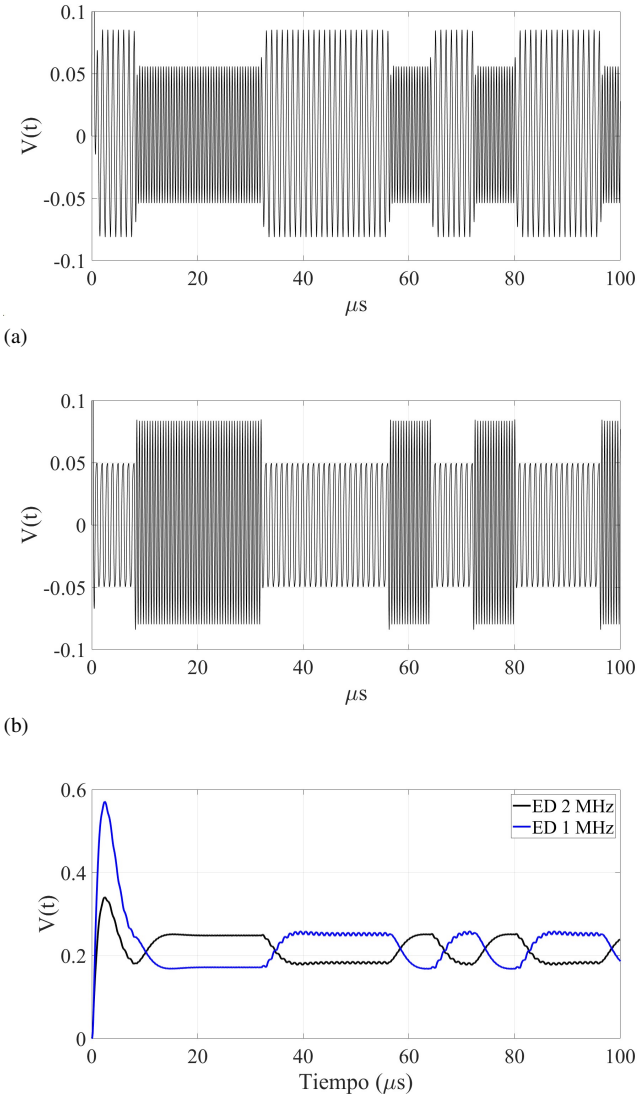

Fig. 14. Demodulator BFSK signals. (a) Output signal of the 1 MHz band-pass filter, (b) Output signal of the 2 MHz band-pass filter, (c) Outputs of envelope detectors for 1 MHz and 2 MHz band-pass filters.

transceiver CppSim description in this work.

The first plot represents the transmitted digital signal, which alternates between two voltage levels: 0 V and 1 V. This is typical of a binary digital system, where the levels represent '0' and '1'. The data could arrive from a digital serialization system or an oversampling converter. The second plot shows the signal received by the receiver after transmission. The received signal recovers the transmitted pattern, indicating the receiver function with a 2.4291 μs time delay which is in good agreement with UWB typical transceivers latency.

D. Performance with Uncertainties

The eye diagram (see Fig. 17) illustrates the transition between these frequencies without noise, forming a pattern that reveals the clarity of the signal. It is important to note that the eye diagram relates to the sub-carrier, meaning that

TABLE II
FUNCTIONAL AND PERFORMANCE COMPARISON OF BEHAVIORAL MODELS FOR FM-UWB SYSTEMS

Characteristics	**[8]**	**[14]**	**[15]**	**[This Work]**
Software	Matlab	Matlab	-	CppSim/Virtuoso
Integration	ADC-TX	TX/RX	TX/RX	TX/RX
Modulation	IR-UWB	FM-UWB	FM-UWB	FM-UWB
Bandwidth	3.5 GHz–4.5 GHz	3.75 GHz–4.25 GHz	3.5 GHz–4 GHz	4 GHz–6 GHz
Baud rate	-	125 kbps	250 kbps	125 kbps
Sub-carrier	-	BFSK	8-PSK	BFSK
Demodulation FM	-	Delay-line, filter, amplifier	Regenerative	Regenerative
FSK/PSK Demodulation	-	-	Phase detector, 3-bit counter	Dual-band pass filter, ED, subtractor

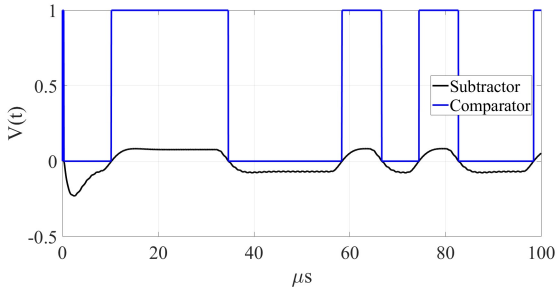

Fig. 15. Subtracting the signals in Fig. 14c and comparing them about 0.

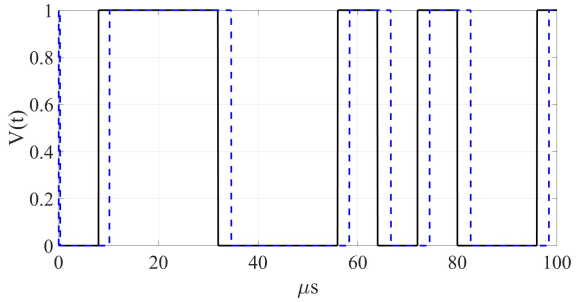

Fig. 16. The transmitted signal is depicted in black, while the received signal is illustrated in blue.

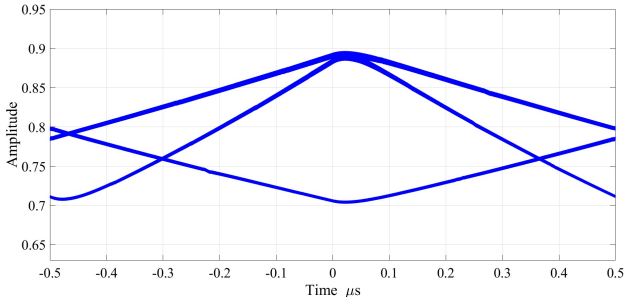

Fig. 17. Eye diagram of the proposed transmitter indicating good timing resolution and low jitter.

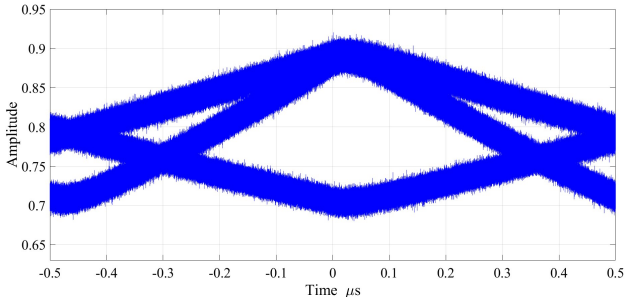

Fig. 18. Eye diagram of the proposed receiver, where the presence of noise reduces signal integrity, but reliable detection is still achieved.

the contributions occur at the maximum frequency of the oscillator. In [16], there is an eye diagram with a waveform similar to the one obtained in this work. The only difference is the oscillation frequency of the sub-carrier, which is $4.125\,\mathrm{MHz}$. In addition, [17] has an eye diagram with OOK modulation, where the eye-opening demonstrates a stable communication system. The noise applied to the system comes mainly from the VCO where a phase noise of $-70\,\mathrm{dBc/Hz}$ was placed. The main characteristics of Fig. 17 obtained are; eye height is $0.194\,58\,\mathrm{V}$, SNL is $4.967\,783$, estimated BER of $8.11x10^{-5}$.

External Gaussian noise was applied to the eye diagram (see Fig. 18) at an SNR of $50\,\mathrm{dB}$ [18], [19]. The following characteristics were obtained: eye height es 0.23, SNL of 3.9431, and BER of $9.91x10^{-5}$.

E. Comparison with similar behavioral descriptions.

Table II summarizes the system-level model and compares it with related works. The behavioral models from [8] and [14] were simulated using the RF-Matlab toolbox, while [15] utilized proprietary software. In this study, we employed CppSim ([9]), which has the significant advantage of being open-source and compatible with Cadence-Virtuoso. This results in lower costs and greater flexibility, enhanced by community-driven improvements.

V. CONCLUSION

The FM-UWB transmission block provides several notable advantages, such as simple circuit design and seamless integration with modern digital systems. On the receiver side, the combination of band-pass filtering, envelope detection, signal subtraction, and comparison effectively minimizes noise, isolates relevant information, and simplifies signal processing. FM-UWB at low data rates achieves a robust receiver architecture. This approach eliminates the need for precise synchronization or complex coherent demodulation processes.

The system demonstrates robustness, ensuring that transmitted and received signals remain consistent despite minor timing variations. This reliability confirms the system's ability to maintain data integrity and synchronization, making it suitable for precise and efficient digital communication.

REFERENCES

[1] United Nations General Assembly, "Transforming our world: the 2030 Agenda for Sustainable Development," 2015. [Online]. Available: https://sdgs.un.org/2030agenda

[2] Federal Communications Commission, "Revision of Part 15 of the Commission's Rules Regarding Ultra-Wideband Transmission Systems," 2002. [Online]. Available: https://www.fcc.gov/document/revision-part-15-commissions-rules-regarding-ultra-wideband-1

[3] R. J. Fontana, *A Brief History of UWB Communications*. Multispectral Solutions, Inc., 2004. [Online]. Available: https://www.ultrawidebandtech.com/history.html

[4] Federal Communications Commission, "FCC Guidelines on Ultra-Wideband Technology," 2020. [Online]. Available: https://www.fcc.gov/engineering-technology/policy-and-rules

[5] "Ultra-Wideband Technology for Wireless Body Area Networks: Opportunities and Challenges," *IEEE Access*, vol. 8, pp. 16031–16042, 2020. doi: 10.1109/ACCESS.2020.2965121

[6] S. Gezici and H. V. Poor, "Localization in Ultra-Wideband Networks: Theory and Practice," *IEEE Signal Processing Magazine*, vol. 22, no. 4, pp. 70–84, 2005. doi: 10.1109/MSP.2005.1458289

[7] B. Wang, H. Song, W. Rhee, and Z. Wang, "Overview of ultra-wideband transceivers—system architectures and applications," *Tsinghua Science and Technology*, vol. 27, no. 3, pp. 481–494, 2022. doi: 10.26599/TST.2021.9010044

[8] A. Diaz-Armendariz, L. A. Sanchez-Gaspariano, V. R. Gonzalez-Diaz, A. I. Bautista-Castillo, J. M. Munoz-Pacheco, and A. Diaz-Sanchez, "Mono-Bit Quantizer $\Sigma\Delta$ Direct-Up Transmitter for UWB Using Simulink RF Blockset," in *Proc. 2019 Int. Conf. on Electronics, Communications and Computers (CONIELECOMP)*, pp. 158–163, 2019. doi: 10.1109/CONIELECOMP.2019.8673255

[9] M. H. Perrott, *A Primer for the CppSim and VppSim Simulation Environments*, 5th ed., 2009. [Online]. Available: https://www.cppsim.com/Manuals/cppsim_vppsim_primer5.pdf (Accessed: 2024-10-10)

[10] C. Enz and V. Kopta, *Ultra-Low Power FM-UWB Transceivers for IoT*, River, 2022. doi: 10.1201/9781003339908

[11] M. Dante, M. Tonolli, V. Raab, M. Casoni, and C. Buratti, "FM-UWB: Towards a Robust, Low-Power Radio for Body Area Networks," in *Proc. 2012 IEEE International Conference on Communications (ICC)*, pp. 3409–3413, 2012. doi: 10.1109/ICC.2012.6363661

[12] L. W. Couch, *Digital and Analog Communication Systems*, 6th ed., Prentice Hall, 2001.

[13] B. Razavi, *RF Microelectronics*, 2nd ed., Pearson Education, Upper Saddle River, NJ, USA, 2012.

[14] J. F. M. Gerrits, J. R. Farserotu, and J. R. Long, "Multipath Behavior of FM-UWB Signals," in *Proc. 2007 IEEE International Conference on Ultra-Wideband*, pp. 162–167, 2007. doi: 10.1109/ICUWB.2007.4380934

[15] D. Liu, F. Chen, W. Rhee, and Z. Wang, "An FM-UWB transceiver with M-PSK subcarrier modulation and regenerative FM demodulation," in *Proc. 2013 IEEE 56th International Midwest Symposium on Circuits and Systems (MWSCAS)*, pp. 936–939, 2013. doi: 10.1109/MWSCAS.2013.6674804

[16] M. Abtahi, M. Mirshafiei, L. A. Rusch, and S. LaRochelle, "An optical realization of a 500 Mb/s UWB transceiver," in *Proc. 2008 IEEE International Conference on Ultra-Wideband*, vol. 1, pp. 133–136, 2008. doi: 10.1109/ICUWB.2008.4653302

[17] J. Bergervoet, H. Kundur, D. M. W. Leenaerts, R. C. H. van de Beek, R. Roovers, G. van der Weide, H. Waite, and S. Aggarwal, "A fully integrated 3-band OFDM UWB transceiver in 0.25/spl mu/m SiGe BiCMOS," in *Proc. IEEE Radio Frequency Integrated Circuits (RFIC) Symposium*, pp. 4 pp.-268, 2006. doi: 10.1109/RFIC.2006.1651142

[18] A. Alshabo, P. J. Vial, M. Ros, D. Stirling, and M. A. B. Sidik, "Ultra Wideband Noise Channel Measurement Using a Vector Network Analyzer," *TELKOMNIKA Telecommunication, Computing, Electronics and Control*, vol. 13, no. 3, pp. 695–702, 2025. doi: 10.12928/telkomnika.v13i3.2095

[19] A. Jiménez Tejero, "Efecto del sistema UWB sobre sistemas de telecomunicaciones con bandas de operación por debajo de los 3 GHz," Proyecto Fin de Carrera, Universidad Autónoma de Madrid, Escuela Politécnica Superior, Octubre 2008.

Juan C. Garcia-Gutierrez received the B.Sc. degree in mechatronics engineering from Benemérita Universidad Autónoma de Puebla (BUAP) in 2021. He collaborated in the characterization of chips at the Circuits and Systems Characterization Laboratory, Faculty of Electronics. At the time, he is studying the M.Sc. degree from Benemérita Universidad Autónoma de Puebla (BUAP). His research interests are systems radio frequency design for wireless communications.

Victor R Gonzalez-Diaz (Senior Member, IEEE) received the M.Sc. and Ph.D. degrees from the National Institute of Astrophysics, Optics and Electronics (INAOE), Puebla, Mexico, in 2005 and 2009, respectively. He collaborated as a Postdoctoral Fellow with the Microsystems Laboratory, University of Pavia, Italy, from 2009 to 2010. He has been a full-time Professor with the Faculty of Electronics, BUAP, Puebla, since 2011. He is currently the Founder and the Head of the Circuits and Systems Characterization Laboratory, Faculty of Electronics. His research interests include the design of analog and mixed-signal integrated circuits focusing on analog-to-digital converter design, frequency synthesizers, and micropower management circuits. He participates as an Associate Editor of IEEE TRANSACTIONS ON CIRCUITS AND SYSTEMS—II: EXPRESS BRIEFS.

Luis A. Sanchez-Gaspariano received the PhD degree in Electronics Sciences from the Instituto Nacional de Astrofísica, Óptica y Electrónica (INAOE), Puebla, Mexico, in 2011. His doctoral work was on the subject of CMOS Power Amplifiers for wireless communications. During 2009 he was a visiting scholar in the Integrated Circuits Design (ICD) group at the University of Twente, in the Netherlands. In 2011 he joined the Electronics and Telecommunications department at the Universidad Politécnica de Puebla, in Puebla, Mexico, where he served as the head of the Electronics group for about seven years. Since 2017 to date, he is with the Electronics Faculty at Benemérita Universidad Autónoma de Puebla (BUAP), in Puebla, Mexico, as a full professor and member of the Photonics and Nanooptics Systems research group. He is a regular member (level-1) of the National Systems for Researchers (SNI), which is a top-level program founded by the Mexican Government through the National Council of Human Studies, Science and Technology (CONAHCyT) from Mexico. He has published over 60 scientific works and regularly serves as a reviewer for high-impact journals. His research focuses on Electronic Design Automation (EDA) tools, analog, mixed-mode, and RF circuit design, and next-generation wireless systems like IoT and 5G, particularly in automotive applications.